RSC Advances

PAPER

View Article Online
View Journal | View Issue

Cite this: *RSC Adv.*, 2020, **10**, 41165

Synthesis of new thienylpicolinamidine derivatives and possible mechanisms of antiproliferative activity†

Mohamed A. Ismail,*[a] Mohamed H. Abdel-Rhman,[a] Ghada A. Abdelwahab,[a] Wafaa S. Hamama,[a] Heba M. El-Shafeai[a] and Wael M. El-Sayed*[b]

Three thienylpicolinamidine derivatives **4a–c** were prepared from their corresponding picolinonitriles **3a–c** on treatment with lithium trimethylsilylamide, $LiN(TMS)_2$, followed by a de-protection step using ethanol/HCl (gas). DFT calculations were used to optimize the geometric structure of the newly synthesized picolinamidines. The comparison of DFT calculated spectral data with the experimental data (^{1}H-NMR and ^{13}C-NMR) showed a good agreement. The *in vitro* antiproliferative activity of the cationic compounds **4a–c** was determined against 60 cancer cell lines representing nine types of cancer. The tested picolinamidines were highly active with compounds **4a** and **4b** eliciting mainly cytotoxic activity with GI values ranging from −7.17 to −86.03. Leukemia (SR and K-562), colon (SW-620 and HT29), and non-small cell lung cancer (NCI-H460) cell lines were the most responsive to the investigated picolinamidines. In particular, 4-methoxyphenyl derivative **4a** showed a profound growth deterring power with GI_{50} of 0.34 μM against SR, 0.43 μM against SW-620, and 0.52 μM against NCI-H460. The three tested picolinamidines elicited potent GI_{50} values against all tested cell lines at low micromolar to sub-micromolar level. The new picolinamidines were selective and did not affect normal human fibroblasts. The selectivity index ranged from 13–21 μM. The novel picolinamidines downregulated the expression of key genes in the cell cycle, *cdk1* and *topoII*, but did not affect *p53* or *txnrd1*. Compounds **4b** and **4c** caused a significant reduction in the concentrations of TopoII and MAPK proteins but were devoid of any effect on the activity of caspase 3. Taken together, these promising anticancer candidates are effective at very low concentrations and safe to normal cells, and most probably work through arresting the cell cycle, and therefore, they deserve further investigations.

Received 15th October 2020
Accepted 4th November 2020

DOI: 10.1039/d0ra08796c

rsc.li/rsc-advances

1. Introduction

Cancer is a fast growing global threat. According to the WHO health observatory report in 2018, about 9.6 million people have died from cancer worldwide. This number is projected to double by 2030. With about 26 million new cancer cases worldwide expected by 2030, cancer may precede cardiovascular diseases in affecting the humans. Although progress has been achieved regarding the 5-year survival, the increase of incidence is still ongoing at a rate exceeding this progress.[1] At present, surgical treatment, combined with radiotherapy and chemotherapy are the main treatments for colorectal cancer.[2,3] Over the recent years, technical advances have led to better response to cancer therapies and survival rates, but still substantial number of patients cannot be cured, develop metastasis, and/or suffer from severe early and late side effects. Therefore, the discovery of new anticancer agents is of great importance.

Pyridine derivatives possess a diverse chemotherapeutic profile as anticancer, antimicrobial, or antiprotozoal agents. The pyridine ring mostly contributes an effective role in the pharmacokinetic properties of these biologically active compounds.[4–8] Furanylnicotinamidine derivatives have been reported for their potent antiproliferative activity.[4] Symmetrical furanylnicotinamidine compound DB829 has successfully passed the preclinical studies as antitrypanosomal agent.[5–7] Cationic arylchalcophenes have been reported for their wide range of biological activities.[9–13] Cationic arylthiophene derivatives have been reported for their anticancer activity.[14,15] Recently, a bithiophene-fluorobenzamidine compound showed a very promising antitumor activity against colorectal cancer in rats reducing the incidence and multiplicity of polyps without causing hepato- or nephro-toxicity.[16]

Based on the biological importance of the reported pyridines and cationic arylthiophenes, three picolinamidine derivatives including methoxy and chloro-substituted phenyl moiety were

[a]*Department of Chemistry, Faculty of Science, Mansoura University, Mansoura 35516, Egypt. E-mail: mismail@mans.edu.eg*

[b]*Department of Zoology, Faculty of Science, University of Ain Shams, Abbassia 11566, Cairo, Egypt. E-mail: wael_farag@sci.asu.edu.eg*

† Electronic supplementary information (ESI) available. See DOI: 10.1039/d0ra08796c

synthesized and evaluated for *in vitro* antiproliferative activity against 60 cancer cell lines at the National Cancer Institute (NCI). The most responsive two types were leukemia and colon cancer cell lines (six cell lines for leukemia & seven for colon cancer). The selectivity of these compounds was assessed using WI-38 normal human fibroblasts. To understand the molecular pathways through which these compounds could exert their anticancer activity, the effect of these compounds on the expression of some of the key genes and proteins in the cell cycle and apoptosis was studied in HepG2 cells. These genes and proteins include p53, cyclin-dependent kinase 1 (cdk1), caspase 3, topoisomerase II (topo II), thioredoxin reductase 1 (txnrd1), and p38 mitogen-activated protein kinase (MAPK). Also, the quantum chemical calculation at DFT/B3LYP level was studied to investigate the structural, electronic, and spectral properties of the new picolinamidine derivatives.

2. Experimental

2.1. Chemistry

Melting points were measured in degree centigrade on Gallenkamp apparatus and are uncorrected. The infrared spectra (KBr) were recorded on Thermo Scientific Nicolet iS10 FT-IR spectrometer. Reaction monitoring was made using thin layer chromatography on silica gel pre-coated aluminum sheets (60 F_{254}), and visualized under ultraviolet light. ^{1}H-NMR and ^{13}C-NMR spectra were measured in dimethyl sulfoxide (DMSO-d_6) as a solvent and self-internal reference (2.49 parts per million (ppm) for proton and 39.50 ppm for carbon using 500 MHz JEOL's spectrometer). A GC-MS (Shimadzu Qp-2010 Plus) spectrometer was used for recording mass spectra. The elemental analyses were measured using PerkinElmer 2400 CHN analyzer and were within ±0.4 of the theoretical values.

2.1.1. General methodology for preparation of thienylpicolinonitrile derivatives (3a–c). A mixture of 6-(5-bromothiophen-2-yl)picolinonitrile[17] (663 mg, 2.5 mmol), $Pd(PPh_3)_4$ (100 mg), appropriate phenylboronic acid (3.0 mmol), and anhydrous K_2CO_3 (3 g) in 1,4-dioxane (20 mL) was refluxed with stirring for 12 hours. Where after the reaction mixture was extracted with ethyl acetate (200 mL, 3×) from aqueous ammonia (20 mL). The organic layer was evaporated to dryness under reduced pressure. The resultant solid was recrystallized from ethanol/EtOAc to furnish the desired thienylpicolinonitrile derivative of **3a–c**.

*2.1.1.1. 5-[5-(4-Methoxyphenyl)thiophen-2-yl]picolinonitrile (**3a**).* Compound **3a** was obtained in 66% yield as a golden-yellow solid, mp 153–154 °C. R_f = 0.40, petroleum ether (60–80 °C)–EtOAc (7 : 3). IR (KBr) ν'/cm^{-1}; 3080, 2957 (CH, stretch), 2228 (CN, stretch), 1602, 1573, 1507 (C=N, C=C, stretch) cm^{-1}. ^{1}H-NMR (DMSO-d_6); δ/ppm = 3.80 (s, 3H, OCH_3), 7.02 (d, J = 8.5 Hz, 2H), 7.56 (d, J = 4.0 Hz, 1H of thiophene ring), 7.66 (d, J = 8.5 Hz, 2H), 7.86 (d, J = 4.0 Hz, 1H of thiophene ring), 8.05 (d, J = 8.5 Hz, 1H of pyridyl ring), 8.26 (dd, J = 8.5, 2.0 Hz, 1H of pyridyl ring), 9.09 (d, J = 2.0 Hz, 1H of pyridyl ring). ^{13}C-NMR; δ 55.32, 114.70 (2C), 117.70, 124.36, 125.57, 126.98 (2C), 128.96, 129.33, 130.04, 132.76, 133.08, 135.56, 146.36, 147.19, 159.57. MS (EI) m/z (rel. int.); 292 (M^+, 100), 277 (M^+–CH_3, 63). Anal. calcd for: $C_{17}H_{12}N_2OS$ (292.35): C, 69.84; H, 4.14; N, 9.58 found: C, 69.73; H, 4.20; N, 9.37%.

*2.1.1.2. 5-[5-(3-Chloro-4-methoxyphenyl)thiophen-2-yl]picolinonitrile (**3b**).* Compound **3b** was obtained in 71% yield as a yellow solid, mp 195–196.5 °C. R_f = 0.41, petroleum ether (60–80 °C)–EtOAc (7 : 3). IR (KBr) ν'/cm^{-1}; 3050, 2945 (CH, stretch), 2225 (CN, stretch), 1603, 1573, 1544 (C=C, stretch) cm^{-1}. ^{1}H-NMR (DMSO-d_6); δ/ppm = 3.89 (s, 3H, OCH_3), 7.23 (d, J = 8.5 Hz, 1H), 7.64–7.67 (m, 2H), 7.83 (d, J = 2.5 Hz, 1H), 7.88 (d, J = 4.0 Hz, 1H of thiophene ring), 8.06 (d, J = 8.5 Hz, 1H), 8.28 (dd, J = 8.5, 2.0 Hz, 1H), 9.10 (d, J = 2.0 Hz, 1H of pyridyl ring). MS (EI) m/z (rel. int.); 326, 328 (M^+, 100, 38; chlorine isotopes), 311, 313 (M^+–CH_3, 82, 31; chlorine isotopes). Anal. calcd for: $C_{17}H_{11}ClN_2OS$ (326.80): C, 62.48; H, 3.39; N, 8.57 found: C, 62.31; H, 3.52; N, 8.35%.

*2.1.1.3. 5-(5-(3,4,5-Trimethoxyphenyl)thiophen-2-yl)picolinonitrile (**3c**).* Compound **3c** was obtained in 84% yield as a yellow solid, mp 170–171 °C. R_f = 0.22, petroleum ether (60–80 °C)–EtOAc (7 : 3). IR (KBr) ν'/cm^{-1}; 3060, 2934 (CH, stretch), 2226 (CN, stretch), 1579, 1509 (C=C, stretch) cm^{-1}. ^{1}H-NMR (DMSO-d_6); δ/ppm = 3.69 (s, 3H, OCH_3), 3.86 (s, 6H, 2 × OCH_3), 6.98 (s, 2H), 7.67 (d, J = 4.0 Hz, 1H of thiophene ring), 7.91 (d, J = 4.0 Hz, 1H of thiophene ring), 8.06 (d, J = 8.5 Hz, 1H of pyridyl ring), 8.30 (dd, J = 8.5, 2.0 Hz, 1H of pyridyl ring), 9.11 (d, 2.0 Hz, 1H of pyridyl ring). ^{13}C-NMR; δ 56.07 (2C), 60.15, 103.17 (2C), 117.63, 125.71, 128.62, 128.82, 129.33, 130.21, 132.88, 132.96, 136.40, 137.89, 146.36, 147.22, 153.36 (2C). MS (EI) m/z (rel. int.); 352 (M^+, 100), 337 (M^+–CH_3, 83). Anal. calcd for: $C_{19}H_{16}N_2O_3S$ (352.40): C, 64.76; H, 4.58; N, 7.95 found: C, 64.52; H, 4.65; N, 7.72%.

2.1.2. General methodology for preparation of thienylpicolinamidine derivatives (4a–c). Each thienylpicolinonitrile derivative of **3a–c** (1.5 mmol) was treated with $LiN(TMS)_2$ (1 M solution in THF, 8 mL, 8 mmol) and the reaction was allowed to stir overnight. Then, ethanolic–HCl (gas) solution (12 mL, 1.25 M) was added dropwise with cooling, until a precipitate was formed. The mixture was left to stir at ambient temperature for 6 hours and the resultant solid was collected through filtration after it was diluted with ether. The crude solid of thienylpicolinamidine derivative was neutralized with 1 N NaOH followed by filtration. The monoamidine free bases were converted to their corresponding hydrochloride salts of the target thienylpicolinamidines **4a–c** using ethanolic–HCl (gas) solution.

*2.1.2.1. 5-[5-(4-Methoxyphenyl)thiophen-2-yl]picolinamidine hydrochloride salt (**4a**).* Compound **4a** was obtained in 82% yield as a yellowish-brown solid, mp 257–259 °C. IR (KBr) ν'/cm^{-1}; 3430, 3383, 3274 (NH, stretch), 3071, 2963 (CH, stretch), 1679, 1605, 1577 (C=N & C=C, stretch) cm^{-1}. ^{1}H-NMR (DMSO-d_6); δ/ppm = 3.79 (s, 3H, OCH_3), 7.02 (d, J = 8.5 Hz, 2H Ar of 4-methoxyphenyl-), 7.56 (d, J = 4.0 Hz, 1H of thiophene ring), 7.67 (d, J = 8.5 Hz, 2H Ar of 4-methoxyphenyl-), 7.92 (d, J = 4.0 Hz, 1H of thiophene ring), 8.37 (d, J = 8.5 Hz, 1H of pyridyl ring), 8.40 (dd, J = 8.5, 2.0 Hz, 1H of pyridyl ring), 9.11 (d, J = 2.0 Hz, 1H of pyridyl ring), 9.39 (s, 2H, NH_2), 9.59 (s, 2H, $^+NH_2$). ^{13}C-NMR; δ 55.32, 114.68 (2C), 123.77, 124.33, 125.58, 126.95 (2C), 128.96, 133.14, 133.77, 135.66, 141.60, 145.62, 146.23, 159.54, 161.43. MS (EI) m/z (rel. int.); 309 (M^+, 100), 294 (M^+–CH_3, 15),

292 (M^+–NH_3, 62). Anal. calcd for: $C_{17}H_{15}N_3OS$-1.0HCl (345.84): C, 59.04; H, 4.66; N, 12.15 found: C, 58.84; H, 4.70; N, 11.91%.

*2.1.2.2. 5-[5-(3-Chloro-4-methoxyphenyl)thiophen-2-yl] picolinamidine hydrochloride salt (**4b**).* Compound **4b** was obtained in 76% yield as a golden-yellow solid, mp 266–267.5 °C. IR (KBr) ν'/cm^{-1}; 3361 (NH, stretch), 3059, 2950 (CH, stretch), 1683, 1579, 1531 (C=N & C=C, stretch) cm^{-1}. ^{1}H-NMR (DMSO-d_6); δ/ppm = 3.89 (s, 3H, OCH_3), 7.24 (d, J = 8.5 Hz, 1H), 7.65–7.67 (m, 2H), 7.83 (d, J = 2.0 Hz, 1H), 7.94 (d, J = 4.0 Hz, 1H of thiophene ring), 8.36 (d, J = 8.5 Hz, 1H), 8.41 (dd, J = 8.5, 2.0 Hz, 1H), 9.12 (d, J = 2.0 Hz, 1H), 9.38 (s, 2H, NH_2), 9.59 (s, 2H, $^+NH_2$). ^{13}C-NMR; δ 56.35, 113.44, 121.88, 123.73, 125.37, 125.62, 126.53, 126.68, 129.00, 133.33, 133.60, 136.45, 141.85, 144.44, 145.71, 154.58, 161.31. MS (EI) m/z (rel. int.); 343, 345 (M^+, 100, 43: chlorine isotopes), 328, 330 (M^+–CH_3, 43, 9: chlorine isotopes), 326, 328 (M^+–NH_3, 72, 43: chlorine isotopes). Anal. calcd for: $C_{17}H_{14}ClN_3OS$-1.0HCl (380.29): C, 53.69; H, 3.98; N, 11.05 found: C, 53.43; H, 4.10; N, 10.79%.

*2.1.2.3. 5-[5-(3,4,5-Trimethoxyphenyl)thiophen-2-yl] picolinamidine hydrochloride salt (**4c**).* Compound **4c** was obtained in 75% yield as a golden-yellow solid, mp 280–281.5 °C. IR (KBr) ν'/cm^{-1}; 3426, 3250 (NH, stretch), 3054, 2990, 2954 (CH, stretch), 1684, 1632, 1582 (C=N & C=C, stretch) cm^{-1}. ^{1}H-NMR (DMSO-d_6); δ/ppm = 3.69 (s, 3H, *para* OCH_3), 3.86 (s, 6H, *meta* 2 OCH_3), 6.99 (s, 2H), 7.70 (d, J = 4.0 Hz, 1H of thiophene ring), 7.97 (d, J = 4.0 Hz, 1H of thiophene ring), 8.38 (d, J = 8.5 Hz, 1H of pyridyl ring), 8.44 (dd, J = 8.5, 2.0 Hz, 1H of pyridyl ring), 9.14 (d, 2.0 Hz, 1H of pyridyl ring), 9.41 (s, 2H, NH_2), 9.60 (s, 2H, $^+NH_2$). ^{13}C-NMR; δ 56.09 (2C), 60.16, 103.17 (2C), 123.76, 125.73, 128.67, 128.82, 133.33, 133.69, 136.54, 137.89, 141.82, 145.69, 146.26, 153.37 (2C), 161.37. MS (EI) m/z (rel. int.); 369 (M^+, 100), 354 (M^+–CH_3, 65), 352 (M^+–NH_3, 37), 337 (35). Anal. calcd for $C_{19}H_{19}N_3O_3S$-1.0HCl (405.89): C, 56.22; H, 4.97; N, 10.35 found: C, 55.98; H, 4.99; N, 10.12%.

2.2. Computational studies

Quantum chemical calculations were achieved using Gaussian 09W program[18] to optimize the geometry at DFT/B3LYP level[19–21] with standard 6-311++G(d,p) basis set. In DMSO, ^{1}H and ^{13}C-NMR chemical shifts were calculated by the gauge-invariant atomic orbital (GIAO) method[22] by polarizable continuum model using the integral equation formalism variant (IEF-PCM).[23,24] The NMR spectral data were assigned by GaussView 6.0 program,[25] using corresponding TMS shielding calculated at the same theoretical levels as the reference. Fukui indices have been calculated using DMol3 module of Materials Studio package from Accelrys Inc.[26] The B3LYP functions have been used with a double numeric plus polarization (DNP version 3.5) basis set which has comparable accuracy to 6-31G** Gaussian basis set.[27]

2.3. Biology

2.3.1. *In vitro* antiproliferative screening. The antiproliferative activity of the three thienylpicolinamidine derivatives **4a–c** was tested by the NCI (USA). The studied picolinamidines were initially evaluated in a single dose (10 μM) assay and because they were promising, the picolinamidines were examined in a five-dose screen study against the standard NCI panel of 60 cancer cell lines. The cell viability or growth was estimated adopting the previously published standard methods.[28–30]

2.3.2. Cytotoxicity in normal cells: (MTT assay). The cytotoxic activity of picolinamidines **4a**, **4b**, and **4c** (0.5–100 μM) against the growth of human normal fibroblasts (WI-38) was investigated using the MTT assay as described elsewhere.[28] The cells, bovine serum, trypsin, and media were obtained from the American Type Culture Collection (ATCC; Manassas, VA, USA). The cells were incubated with the compounds for 48 h, then MTT was added and further incubation for 4 h was performed. DMSO was added to dissolve the formazan formed and the optical density was measured at 570 nm. The data are expressed as mean ± SEM for two independent experiments.

2.3.3. Assessment of the expression of *p53*, *caspase-3*, *cdk1 topoisomerase II*, and *txnrd1* by real time PCR. The HepG2 cells were incubated with **4a**, **4b**, and **4c** at the GI_{50} concentrations in DMSO for 8 h. TRIzol reagent (Sigma, St. Louis, MO, USA) was used for the total RNA extraction. Specific primers (Table S1†) for *p53*, *cyclin-dependent kinase 1* (*cdk1*), *caspase-3*, *topoisomerase II* (*topoII*), *thioredoxin reducatse 1* (*txnrd1*), were used in reverse transcription (RT) and q-PCR. RT and q-PCR were performed as described previously.[31] Glyceraldehyde-3-phosphate dehydrogenase (GAPDH) was used as a house-keeping gene. The Maxima SYBR Green qPCR Master Mix was obtained from Bioline (London, UK). Every sample (n = 3) was analyzed in triplicate. The $^{\Delta\Delta}$Ct (cycle threshold, Ct) method was employed to estimate the differences in gene expression between groups after normalization against GAPDH of the same sample.[32] The data were expressed as fold change as compared to the untreated cells.

2.3.3.1. Effect of the new picolinamidine derivatives on p38 mitogen-activated protein kinase (MAPK) and topoisomerase II (Topo II). The concentration of MAPK and Topo II was determined in HepG2 cells after treatment with doxorubicin and the novel compounds (**4a**, **4b**, and **4c**) based on the sandwich ELISA methods using kits from Invitrogen (Carlsbad, CA, USA) and MyBioSource (San Diego, CA, USA), respectively.

2.3.3.2. Measurement of the active cleaved caspase 3 activity. The activity of the cleaved caspase-3 was determined in HepG2 cells after incubation with the GI_{50} concentration of compounds **4a**, **4b**, and **4c** for 12 hours has described elsewhere[33] using kit obtained from Abcam (UK).

3. Results and discussion

3.1. Chemistry

The preparation of the new thienylpicolinamidines **4a–c** (Fig. 1) begins with Suzuki coupling reaction of bromothienyl derivative **1**[17] with the appropriate phenylboronic acid **2a–c** to afford thienylpicolinonitriles **3a–c**. The new picolinonitriles **3a–c** were converted to the target thienylpicolinamidines **4a–c** by the action of $LiN(TMS)_2$, followed by de-protection with hydrogen chloride and subsequent neutralization with NaOH. Picolinamidines hydrochloride salts were prepared by treatment of the

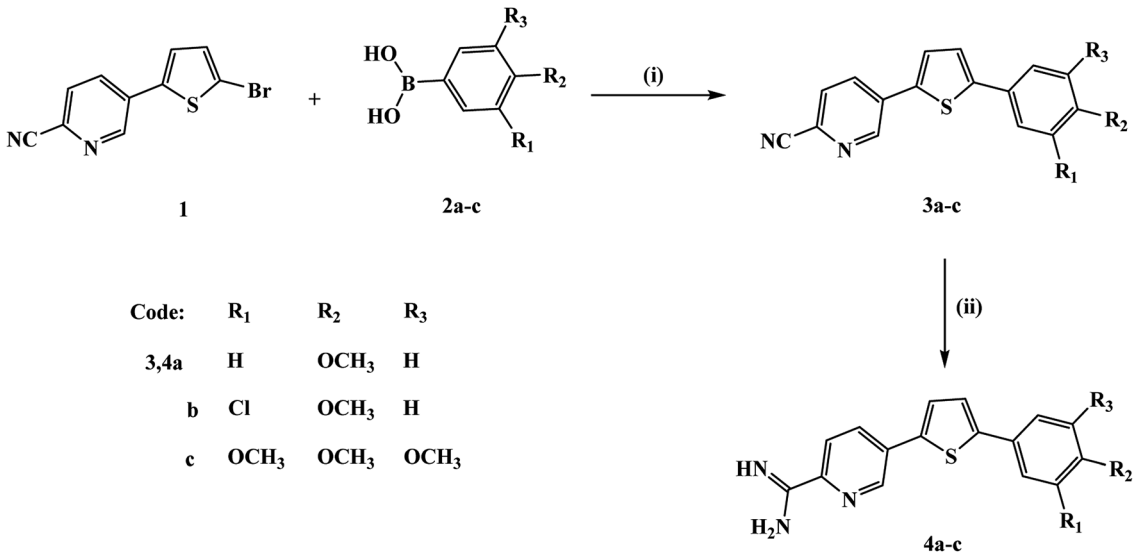

Code:	R_1	R_2	R_3
3,4a	H	OCH_3	H
b	Cl	OCH_3	H
c	OCH_3	OCH_3	OCH_3

Fig. 1 Synthesis scheme for the new thienylpicolinamidine derivatives. Reagents and conditions: (i) $Pd(PPh_3)_4$, anhydrous K_2CO_3, 1,4-dioxane; (ii) (a) $LiN(TMS)_2$, (b) ethanol/HCl (gas).

proper free base of monoamidines with hydrogen chloride in ethanol.

The structures of the new thienylpicolinonitriles **3a–c** and thienylpicolinamidine derivatives **4a–c** were assigned based on their spectral and elemental analyses. The IR spectra of all mononitriles **3a–c** confirmed the appearance of nitrile group in each case with stretching vibrations values of 2228, 2225, and 2226 cm^{-1}, respectively. Whereas, the IR spectra of all monoamidines indicated the disappearance of the nitrile group in each case and displayed new peaks corresponding for N–H stretching vibrations (ν' 3430, 3383 & 3274 cm^{-1} for compound **4a**). ^1H NMR spectra of all monoamidines showed the characteristic signals corresponding to the cationic amidine group and were deuterium exchangeable. Thus, ^1H NMR spectrum of monocationic compound **4a** showed two singlet signals at δ 9.39 (2H) and 9.59 (2H) referring to the cationic amidine group, the presence of ABX system splitting pattern for three protons of 2,5-disubstituted pyridyl moiety, two doublet signals of thiophene ring coupling at δ 7.56 (1H), 7.92 (1H), in addition to three signals; one singlet signal at δ 3.79 (1 × OCH_3), two aromatic doublets at δ 7.02 & 7.67 ppm of AA′BB′ system corresponding to 4-methoxyphenyl moiety. The carbon skeleton of compound **4a** was confirmed by the presence of 15 carbon-lines in its ^{13}C NMR spectrum with two characteristic carbon signals at δ 55.32 (for methoxy carbon), and 161.43 (for amidinic carbon). Moreover, picolinamidine derivative **4a** mass spectrum gave a *m*/*z* peak at 309 referring to its molecular ion peak (M^+), and *m*/*z* peak at 292 corresponding for a fragment produced from the loss a molecule of ammonia. The structure determination of monocationic compound **4c** was confirmed by its ^1H NMR spectrum which displayed two singlets at δ 9.40 (2H, NH_2) & 9.60 (2H, $^+NH_2$) characteristic for the amidinic group, splitting pattern of 2,5-disubstituted pyridyl moiety confirmed by the presence of ABX system (one doublet of doublet at δ 8.44, one large doublet signal at δ 8.38, and small doublet signal at δ 9.14), along with two doublet signals of thiophene ring at δ 7.70 (1H), 7.97 (1H), in addition to three singlet signals at δ 3.69 (1 × OCH_3), 3.86 (2 × OCH_3), 6.99 (2H) referring to 3,4,5-trimethoxyphenyl moiety. The carbon skeleton of **4c** was confirmed by its ^{13}C NMR spectrum with three characteristic carbon signals at δ 56.09 (carbon of *para* methoxy), δ 60.16 (carbons of two equivalent *meta* methoxy groups), and 161.37 (amidinic carbon). Mass fragmentation of picolinamidine derivative **4c** was inconsistent with the mass fragmentation of its nicotinamidine analogue.[34] Compound **4c** gave a *m*/*z* peak at 369 of its molecular ion peak (M^+), *m*/*z* peak at 354 corresponding for a fragment produced from the loss of a methyl group, and *m*/*z* peak at 352 corresponding for a fragment produced from the loss of a molecule of ammonia, in addition to a fragment with *m*/*z* peak at 337 due to the loss of a methyl group and a molecule of ammonia.

3.2. Computational studies

The difficulty to obtain a single crystal of the newly synthesized cationic picolinamidine derivatives promoted us to carry out quantum chemical calculation at DFT/B3LYP level to investigate their structural, electronic and spectral properties.

3.2.1. Geometrical parameters. The DFT optimized structures of the cationic picolinamidine derivatives **4a–c** with numbered atoms were shown in Fig. S1.† The DFT bond length data were found to be longer than the corresponding X-ray reported values by only 0.01–0.1 Å (ref. 35–38) (Table S2†) which may have been attributed to the DFT calculations, a single molecule in gaseous state was considered and so no intermolecular coulombic interactions, while the X-ray obtained for molecules in solid state interacting in crystal lattice.[39]

The dihedral angle data of the cationic picolinamidines **4a–c** showed that the pyridyl ring was titled on the thienyl moiety plane by 3.00–4.50°, *i.e.* in 3-chloro-4-methoxyphenyl derivative

4b, S(5)–C(4)–C(7)–C(13) = 4.37° (Table S3†). Moreover, the amidinic group and pyridyl ring of 4-methoxyphenyl derivative **4a** exhibited ~1.30° for C(14)–C(15)–C(18)–N(20) and C(14)–C(15)–C(18)–N(19) while in 3-chloro-4-methoxyphenyl derivative **4b** and 3,4,5-trimethoxyphenyl derivative **4c**, these angles were in 0.14–0.32° range. Furthermore, the data indicated that the phenyl ring is more titled on thienyl moiety than pyridyl one where the S(5)–C(1)–C(6)–C(8) is ~20.25° for compounds **4a** and **4b** while it reaches ~24.5° in compound **4c**.

Both thienyl and phenyl rings bond angle data of the investigated cationic picolinamidines almost coincided with those obtained from X-ray single crystal of analogue compounds.[35–38] For example, cationic compound **4c** data showed that C(4)–S(5)–C(1), C(4)–C(3)–C(2) and C(9)–C(8)–C(6) angles were 92.40, 113.94 and 121.15°, where their X-ray values were 92.8, 112.6–113.4 and 119.9–120.0°,[35–38] respectively. Meanwhile, the pyridyl ring exhibited a little deviation from the X-ray values ranged from 0.47° to 2.67°. For instance, in case of cationic compound **4a**, the angles C(17)–N(16)–C(15) and C(17)–C(7)–C(13) were 119.34 and 115.63° while the corresponding reported values were 118.5 and 118.3–122.1°,[35–38] respectively. The cationic amidine bond angle H–N^+–H and H–N–H were ~116.88 and 120.40°, respectively. Comparison with the corresponding X-ray reported values indicated a difference by ±3.81° for both angles[35–38] (Table S4†).

3.2.2. Frontier molecular orbitals. Understanding the chemical reactivity toward nucleophilic or electrophilic attack depends mainly on HOMO and LUMO. Within a molecule, the HOMO and LUMO demonstrate the capability to donate and accept an electron,[40] respectively, and their energy explain the ultimate charge transfer.[41,42] Moreover, the HOMO–LUMO energy gap decrease shows the ease of charge transfer interactions, which may be responsible for the bioactivity of the molecules.[43] The 3D plots of frontier orbitals in the optimized geometry denote the red color for positive phase and the green one for the negative phase of wave function as shown in Fig. 2.[44]

As shown in Fig. 2, the thienyl ring is involved in HOMO and LUMO orbitals formation in all derivatives. For example, thienylpicolinamidine derivative **4a**, its HOMO spread mainly over the 4-methoxyphenyl moiety while LUMO orbital is on the pyridyl ring and cationic amidine group. This behaviour was observed in all other derivatives (**4b** and **4c**). The methoxy group and chloro substituents participate strongly in HOMO and slightly in LUMO formation in all derivatives. Thus, it could be concluded that the methoxy or chlorophenyl moieties serve as electron donor sites while the amidinic group at pyridyl moiety acts as electron acceptor. Accordingly, the HOMO–LUMO charge transfer within the **4a–c** derivatives may be expressed as electrons migration from donor site, methoxy or chlorophenyl, to acceptor site, positively charged amidinic group on pyridyl moiety.

As shown in Table 1, the trisubstituted derivative **4c** exhibited the lowest E_{HOMO} −7.94 eV while the chloro derivative **4b** was the highest with −8.17 eV. Moreover, the E_{LUMO} data showed that **4a** and **4c** have the same value, −5.89 eV; while **4b** was a bit higher −5.91 eV. Furthermore, the energy gap data,

Table 1 The HOMO–LUMO energies and chemical reactivity descriptors (eV) of the investigated picolinamidines **4a–c**

Compound	HOMO	LUMO	ΔE_{H-L}	χ	η	δ	ω
4a	−8.08	−5.89	2.19	6.99	1.09	0.91	22.30
4b	−8.17	−5.91	2.27	7.04	1.13	0.88	21.87
4c	−7.94	−5.89	2.05	6.92	1.03	0.98	23.33

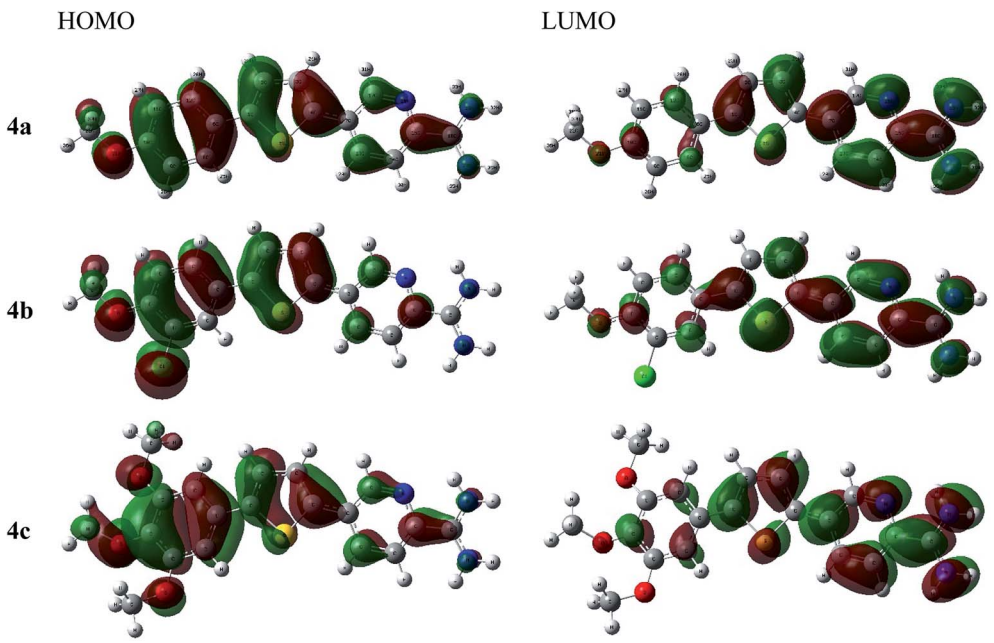

Fig. 2 The frontier molecular orbital of cationic picolinamidines **4a–c**.

$\Delta E_{HOMO-LUMO}$, indicated that the trisubstituted derivative **4c**, 2.05 eV, was the lowest while the disubstituted derivative **4b**, was the highest, 2.27 eV where the three investigated picolinamidines ordered as **4c** < **4a** < **4b**.

The E_{HOMO} and E_{LUMO} have been utilized for determining electronegativity (χ) to evaluate the Lewis acid character, global hardness (η) and softness (δ) as a measure of the charge transfer resistance and the capacity of a molecule to receive electrons, respectively (Table 1). In addition to electrophilicity (ω) which is a measure of energy lowering due to electron flow between HOMO and LUMO[41] where:

$$\chi = -\frac{1}{2}(E_{HOMO} + E_{LUMO})$$

$$\eta = -\frac{1}{2}(E_{HOMO} - E_{LUMO})$$

$$\delta = \frac{1}{\eta}$$

$$\omega = \frac{\chi^2}{2\eta}$$

The data showed that the hardest derivative was **4b** while the softest one was **4c**, where according to softness, the three investigated picolinamidines were ordered as **4b** > **4a** > **4c**. The Mulliken's charges (Table S5†) and Fukui's and relative nucleophilicity indices (Table S6†) were estimated and discussed in details in the ESI section.

3.2.3. NMR spectra. The DFT/B3LYP calculated ^{1}H and ^{13}C-NMR spectral data of the optimized structure for the investigated compounds **4a–c** were shown in Tables S7 and S8† in comparison with their experimental data. The ^{1}H-NMR DFT calculated thienyl protons at positions 3 and 4 were at ~8.24 and ~7.63 ppm, respectively, exhibiting very good agreement with the experimental data with average differences 0.30 and 0.15 ppm where their experimental signals observed at ~7.94 and 7.64 ppm. In addition, the predicted pyridyl and phenyl signals were observed in the ranges of 7.93–9.46 and 7.10–8.30 ppm, respectively, with average differences 0.21 and 0.38 ppm, respectively. The amidinic NH protons in the calculated spectra showed less agreement with the measured spectra by 0.85–3.67 ppm difference which may be attributed to the positive charge and small size of hydrogen atom, therefore their chemical shifts would be more susceptible to intermolecular interactions between the molecules and/or the solvent (Table S7†).[45,46] Excluding the NH's protons, examining the relationship between experimental and calculated chemical shifts showed a linear relationship expressed as $\sigma_{Exp.} = 1.098\ \sigma_{Calcd} - 0.988$ (Fig. 3) with regression coefficient (R^2) 0.962 and root mean square error (RMSE) 0.409.

On the other hand, the ^{13}C-NMR DFT calculated signals for the amidinic carbon atom were observed at ~164.02 ppm while its experimental were at ~161.37 ppm. The methoxy carbon atom in all the derivatives was estimated at ~58.30 ppm

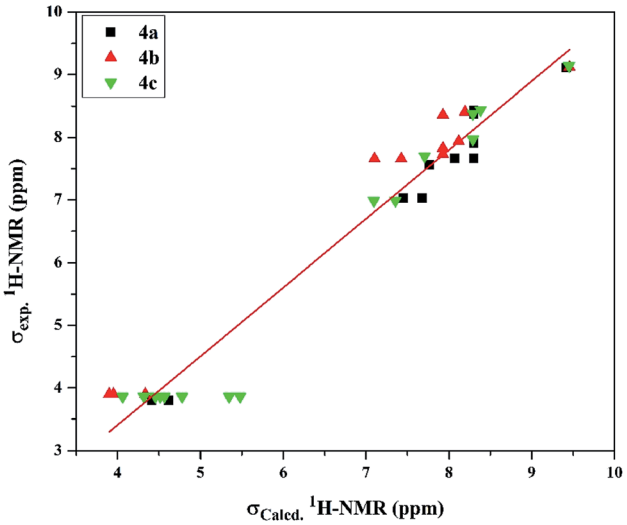

Fig. 3 The linear regression between experimental and DFT calculated ^{1}H NMR chemical shifts of the investigated cationic picolinamidines **4a–c**.

exhibiting average difference 1.89 ppm with the experimental values (Table S8†). The DFT calculation for the pyridyl and phenyl carbons showed signals in the ranges of 126.73–148.78 and 102.64–167.13 ppm, respectively, exhibiting average differences 4.58 and 5.89 ppm, respectively, where the experimental signals observed for the former at 123.73–146.26 ppm and for the latter at 103.17–159.54 ppm. Moreover, the calculated chemical shifts of thienyl carbons, 125.94–164.77 ppm, displayed less agreement with experimental data, 125.58–141.85 ppm, with average difference 10.34 ppm (Table S8†). Examining the relationship between the experimental and calculated chemical shifts showed a linear relationship expressed as $\sigma_{Exp.} = 7.157 + 0.909\ \sigma_{Calcd}$ with regression coefficient (R^2) 0.934 and root mean square error (RMSE) 6.791 (Fig. 4).

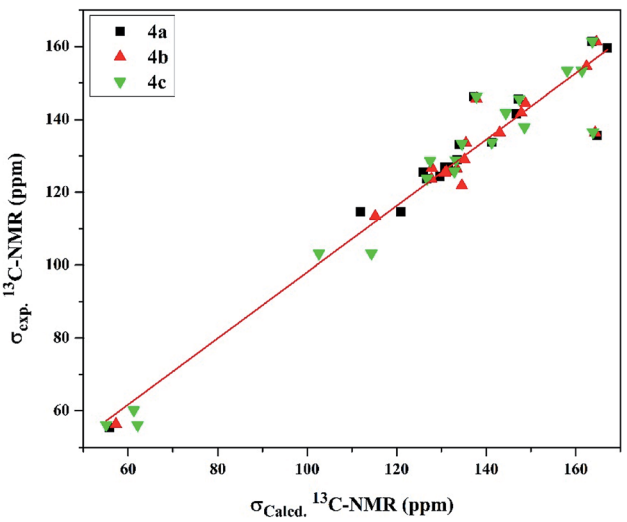

Fig. 4 The linear regression between experimental and DFT calculated ^{13}C NMR chemical shifts of the investigated cationic picolinamidines **4a–c**.

Table 2 *In vitro* percent growth inhibition of the new picolinamidines **4a–c** at a single dose of 10 μM

Leukemia	4a	4b	4c	Colon cancer	4a	4b	4c
CCRF-CEM	−43.35	−48.98	89.10	COLO 205	−52.23	−56.05	NT
HL-60 (TB)	−47.33	−48.71	−40.59	HCC-2998	−44.90	−43.85	87.93
K-562	−26.99	−29.78	94.42	HCT-116	−60.38	−65.49	99.05
MOLT-4	−53.72	−49.30	76.19	HCT-15	−76.97	−77.39	78.61
RPMI-8226	−41.90	−45.37	NT	HT29	−43.08	97.48	85.79
SR	99.71	−7.17	93.69	KM12	−73.71	−86.03	50.93
				SW-620	−65.69	−79.80	70.82

3.3. Biology

Three thienylpicolinamidine derivatives **4a–c** were evaluated for their *in vitro* antiproliferative activity against nine types of cancer cell lines *viz* leukemia, prostate, non-small cell lung, melanoma, colon, ovarian, CNS, renal, and breast cancer at the NCI, USA. First, the chosen compounds were evaluated at an initial high dose of 10 μM. Mean percent growth inhibition (MPGI) of 4-methoxyphenyl derivative **4a** (−28.84) and 3-chloro-4-methoxyphenyl derivative **4b** (−19.95) showed cytotoxic activities. Whereas, 3,4,5-trimethoxyphenyl derivative **4c** (52.58) was cytostatic in action. The individual percent growth inhibition results for the initial screening of the three tested picolinamidines **4a–c** against the most responsive two types of cancer (13 cancer cell lines; six subtypes for leukemia and seven for colon cancer) are presented in Table 2. The tested picolinamidines were highly active with compounds **4a** and **4b** eliciting cytotoxic activity with GI% values ranging from −7.17 to −86.03, and cytostatic activity with 99.71 inhibition for compound **4a** against SR leukemia cancer cell line and 97.48 inhibition for compound **4b** against HT29 colon cancer cell line. Whereas, compound **4c** showed mainly cytostatic activity against all tested cell lines with inhibition activity ranging from 50.93 to 99.05, except for HL-60 (TB) for which **4c** was cytotoxic with GI% of −40.59.

According to the NCI protocol, the compounds showing high antiproliferative activity in the initial screen, all test picolinamidines herein, are to be subjected to a five dose screen for determining their GI_{50} values. The individual GI_{50} values of the tested picolinamidines **4a–c** against a panel of cancer cell lines are presented in Table 3. Among the leukemia and colon cancer cell lines, the most responsive two types tested in the five-dose screen, SR and K-562 leukemia cancer cell lines, and SW-620 and HT29 colon cancer cell lines were the most responsive cell lines. In specific, the most active compound was 4-methoxyphenyl derivative **4a** that showed a profound growth deterring power with an GI_{50} of 0.34 μM against SR and 0.43 μM against SW-620, with an LC_{50} of >100 μM and 4.98 μM, respectively. Furthermore, picolinamidine **4a** exhibited GI_{50} of 0.52 μM against NCI-H460 (non-small cell lung cancer). The 3-chloro-4-methoxyphenyl derivative **4b** comes second with GI_{50} of 0.58 against SR and 0.90 μM against K-562 cell lines, with an LC_{50} of >100 μM for both tested cancer cells. 3,4,5-Trimethoxyphenyl derivative **4c** exhibited GI_{50} ranging from 1.37 to 2.78 μM (for Leukemia and colon) and was the least active in the initial screen among the three tested picolinamidines. According to the cut off set by the NCI at 10 μM, all the three picolinamidines are considered active antiproliferative agents against the 60 cell lines (except compound **4c** against ovarian SK-OV-3 cell line).

These *in vitro* results reflect that while all three compounds elicit potent GI_{50} values against all tested cell lines at the low micromolar to sub-micromolar level, the parent compound **4a** stands out for possessing LC_{50} at low micromolar concentration against five of the seven examined colon cancer cell lines (COLO 205, HCC-2998, HCT-15, KM12, SW-620 with LC_{50} values of 8.13, 6.38, 5.71, 6.03, and 4.98 μM, respectively). On the other hand, picolinamidine derivative **4c** (possessing three methoxy groups on the phenyl ring) demonstrated somewhat better LC_{50} values

Table 3 *In vitro* anti-proliferative activity of the new picolinamidines **4a–c** against a panel of 60 cell lines at five dose level[a,b]

Leukemia	4a	4b	4c	Colon cancer	4a	4b	4c
CCRF-CEM	1.43	1.18	2.49	COLO 205	1.89	1.94	1.60
HL-60 (TB)	1.78	1.66	1.87	HCC-2998	1.82	1.86	2.00
K-562	1.09	0.90	1.39	HCT-116	1.62	1.82	1.47
MOLT-4	1.90	1.72	2.53	HCT-15	1.27	1.57	2.18
RPMI-8226	2.13	2.25	1.67	HT29	0.88	1.35	1.37
SR	0.34	0.58	2.48	KM12	1.81	1.81	2.78
				SW-620	0.43	1.79	2.09

[a] Data represent GI_{50} in μM against the tested cell lines. [b] This table includes the data for the most two responsive types of cancer (for the full data of the nine types of cancer, see Table S9 ESI).

Table 4 Median GI_{50}, TGI and LC_{50} (μM) of the new picolinamidines **4a–c** against a panel of 60 cell lines at five dose level

MG-MID[a]	4a	4b	4c
GI_{50}[b]	1.62	1.73	2.39
TGI[c]	3.31	3.54	6.16
LC_{50}[d]	8.12	8.31	19.49

[a] MG-MID = mean graph midpoint representing mean sensitivity of all examined cell lines to the test compound. [b] GI_{50} = compound concentration causing 50% growth inhibition of tested cells. [c] TGI = compound concentration causing 100% growth inhibition of tested cells. [d] LC_{50} = compound concentration causing 50% lethality of tested cells.

Table 5 *In vitro* cytotoxicity (IC_{50} in μM) of the new picolinamidines **4a–c** against WI-38 and their selectivity index (SI)[a]

Compounds	WI38	SI[c]
Dox	2.9 ± 0.8^b	NA
4a	21.1 ± 3.1^b	13.0
4b	23.7 ± 2.5^b	13.7
4c	51.3 ± 9.0	21.5

[a] The viability of the cells was measured after 48 h of incubation with different concentrations of the investigated compounds by MTT assay. The dose–response curves from as the mean of two parallel experiments were used to determine the IC_{50}; three wells were assigned for every concentration. Doxorubicin (**Dox**) was used as a positive control. The data are presented as mean ± SEM. [b] Significant toxicity as compared to the untreated cells. [c] SI: selectivity index = WI-38 IC_{50}/median GI_{50}.

in both leukemia and colon cancer (HL-60, RPMI-8226, COLO 205, HCC-2998 and HCT-116 with LC_{50} values of 9.44, 9.40, 6.66, 7.61, and 5.60 μM, respectively). Finally, the *m*-chloro substitution at the phenyl ring exemplified by analogue **4b** led to relatively similar growth inhibition profile to that displayed by the parent derivative **4a**, yet it led the compound to have much higher LC_{50} values against all the tested cell lines with the exception of KM12 and SW-620 colon cancer cell lines.

Table 4 presents the median values of GI_{50}, TGI and LC_{50} for the investigated picolinamidine compounds **4a–c**. Compound **4a** was the most active compound giving median GI_{50} values at 1.62 μM. Trimethoxyphenyl derivative **4c** was the least potent growth inhibitor (GI_{50} and TGI values of 2.39 and 6.16 μM, respectively), moreover, it was the least cytotoxic (LC_{50} of 19.49 μM). The HOMO and LUMO, highest occupied and the lowest unoccupied molecular orbitals, have significant role in understanding the chemical reactivity of the molecule to electronic transport and the establishment of biological activity with intramolecular charge transfer. Moreover, the decrease in the HOMO–LUMO energy gap indicates the ease of charge transfer interactions within the molecule, which may be responsible for the bioactivity of the molecules.[41–43] Linking biology data with $\Delta E_{HOMO-LUMO}$ values herein this manuscript, $\Delta E_{HOMO-LUMO}$ indicated that the trimethoxy derivative **4c**, 2.05 eV, is the lowest while the chloro-methoxy derivative **4b**, is the highest, 2.27 eV where the three investigated picolinamidines were ordered as **4c** < **4a** < **4b**. Whereas, the median GI_{50}'s were ordered as **4c** < **4b** < **4a**, therefore, the previous model is valid for compounds **4a** and **4b**, but not for **4c**. This finding suggests that the biological activity could not be correlated to a single factor but it is the interplay between different factors *e.g.* lipophilicity, interaction with nuclear factors and DNA, fitting to different key growth factors and modulators, ability to induce apoptosis, and others.

The ability of the investigated cationic picolinamidines **4a–c** to discriminate between cancer cell and normal cells is one of the essential goals in the anticancer drug development. Therefore, selectivity index (SI) was determined for the three picolinamidines and ranged from 13.0 to 21.5 fold (Table 5). The most selective compound was **4c** (SI = 21.5). These results support the safety of these picolinamidine derivatives and their selectivity against cancer cells.

3.3.1. The effect of new thienylpicolinamidine derivatives on the expression of key cell cycle and apoptosis genes. The main pathways through which the potential anticancer agents exert their antiproliferative activity include the cell cycle arrest and induction of apoptosis. These molecular mechanisms were investigated in the current study by studying the effect of the thienylpicolinamidines on some essential genes (*p53*, *caspase 3*, *cdk1*, *topoII* and *txnrd1*) in the cell cycle and apoptosis in HepG2 cells. HepG2 cells are highly differentiated and display many of the genotypic features of normal liver cells. They also express all the previous genes in good amounts. The HepG2 cells were treated with the picolinamidine compounds (**4a**, **4b**, and **4c**), as well as doxorubicin, and the expression of the five genes was assessed. Doxorubicin caused significant elevations in *p53* and effector *caspase 3*. Similar effects were reported for doxorubicin in previous studies.[47,48] It also caused a significant downregulation in the expression of *cdk1*, *topoII* and *txnrd1* in agreement with previous publications.[49,50] No picolinamidine derivative significantly affected the expression of *p53* or *txnrd1*. Compounds **4b** and **4c** downregulated the expression of *cdk1* and *topoII* but compound **4c** was superior in the magnitude of downregulation (~70%) compared to the ~50% inhibition caused by **4b**. In addition, **4c** elevated the expression of the effector or executioner *caspase 3*. With the exception of its downregulation of *cdk1*, compound **4a** was devoid of any significant effect on the other genes investigated (Table 6).

p53 (the guardian of the genome) is mutated in more than 50% of human cancer types.[51] It is the main regulator of cell cycle progression and apoptosis. When DNA is damaged, p53 expression increases arresting the cell cycle at the G1/S checkpoint, induces the DNA repair mechanisms, or initiates apoptosis if the damage is severe[52] but apparently, none of the

Table 6 Effect of picolinamidine derivatives **4a–c** (100 nM) on the expression of *p53, cdk1, caspase 3* and *topoII* in HepG2 after 8 h incubation

Treatment	*p53*	*cdk1*	*caspase 3*	*topoII*	*txnrd1*
Fold induction from untreated cells					
DOX	3.14 ± 0.81^a	0.31 ± 0.09^a	4.17 ± 0.91^a	0.47 ± 0.08^a	0.47 ± 0.10^a
4a	1.19 ± 0.43	0.37 ± 0.04^a	1.57 ± 0.76	1.23 ± 0.05	1.32 ± 0.14
4b	1.03 ± 0.08	0.51 ± 0.15^a	1.85 ± 0.11	0.57 ± 0.08^a	1.29 ± 0.13
4c	1.18 ± 0.10	0.30 ± 0.04^a	3.37 ± 0.25^a	0.27 ± 0.02^a	1.07 ± 0.12

[a] Significant difference ($p < 0.05$) as compared to untreated cells. The data are expressed as mean ± SEM for two independent experiments.

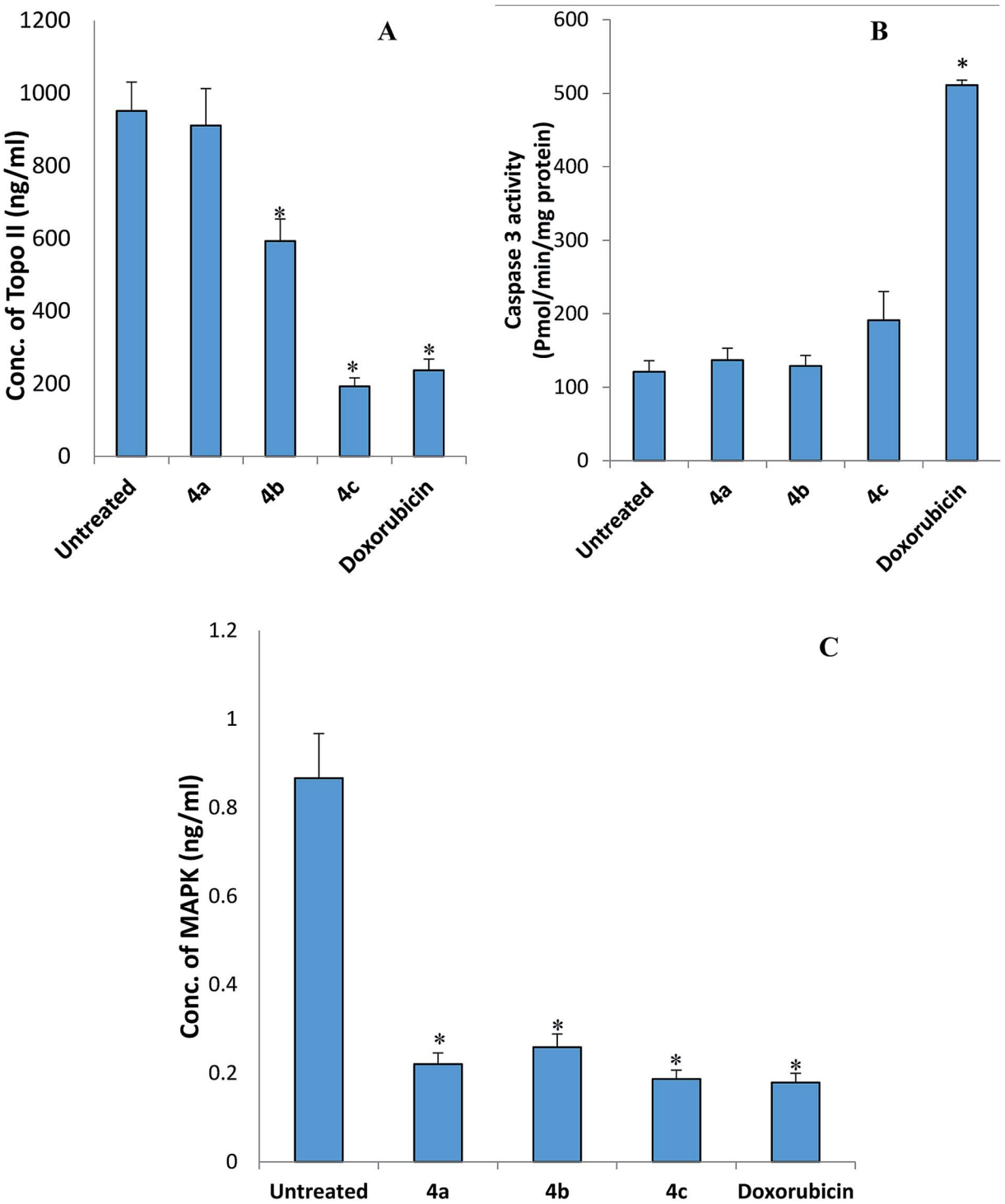

Fig. 5 The effect of the picolinamidine derivatives **4a–c** on (A) topoisomerase II (Topo II) concentration, (B) cleaved caspase 3 activity, and (C) MAPK concentration in HepG2 cells. Each compound has been assigned three wells and the experiment was performed twice. Data are expressed as mean ± SEM. *Significant change compared to untreated cells.

tested picolinamidines acts through this gene. Apoptosis usually occurs through intrinsic or extrinsic pathways. In both pathways caspase 3 is the main execution enzyme.[53]

Cdk1 controls the cell cycle progression to S phase.[54] The downregulation of cdk1 by test compounds **4a**, **4b**, and **4c** suggests the cell cycle arrest. Therefore, we believe that these picolinamidines directly acted on the cdk1 gene without affecting p53, but this assumption needs further investigation. Thioredoxin reductase (Txnrd1) is the only known enzyme that reduces thioredoxin.[55] The role of thioredoxin is very essential

for the structure and activity of proteins, cell growth, and survival. Thioredoxin is responsible for the reduction of proteins and formation of the disulfide bridges. Therefore, this enzyme is upregulated in many types of cancer.[56] Inhibition of txnrd1 leads to cell death.[57] Unfortunately, none of the tested picolinamidines significantly inhibited the expression of this gene.

3.3.2. Inhibitory activity of the new thienylpicolinamidines on p38 mitogen-activated protein kinase (MAPK), topoisomerase II (Topo II), and cleaved caspase 3 activity. The HepG2 cells were treated with the investigated picolinamidines **4a–c** at the IC_{50} concentrations for 8 hours. A four parameter logistic curve-fit was used for constructing the standard curve. The complexity of post-transcription processing of the mRNA and translation of proteins is responsible for the lack of a linear correlation between gene expression and protein expression. Many proteins are secreted as non-functional proteins that need further processing or activation; caspase 3 exists as inactive procaspase 3. Therefore, measuring the activity of the cleaved caspase 3 is the best indication of occurrence of apoptosis. None of the tested picolinamidines affected the activity of the cleaved active caspase 3 although **4c** elevated the expression of the gene but the ~60% increase in the enzyme activity caused by **4c** did not achieve statistical significance (Fig. 5). Compounds **4b** and **4c** in addition to doxorubicin were able to significantly downregulate the concentration of Topo II protein in consistence with their effects on the gene and again **4c** was superior to **4b** in this effect. In a similar scenario, all compounds investigated caused a significant reduction in the concentration of MAPK protein (Fig. 5). Many kinases including MAP kinases are involved in cell proliferation, gene expression, and apoptosis. Therefore, these enzymes become the targets for many anticancer agents. Sorafenib, an approved FDA anticancer agent, is a MAPK inhibitor.[58] Topo II induces the double stranded breaks of DNA and therefore prevents the DNA tangling. This enzyme is essential for the DNA replication and cell division.[59] Nowadays, many potential anticancer agents are investigated as inhibitors of Topo II.[60] The selected reference drug in the current study, doxorubicin is known to arrest the cell cycle and block Topo II, which is the proposed mechanism of action of the new thienylpicolinamidines described in this study.

4. Conclusions

The frontier molecular orbitals of the new thienylpicolinamidines **4a–c**, the energy gap data, $\Delta E_{HOMO-LUMO}$, indicated that the trimethoxy derivative **4c**, is the lowest while the chloromethoxy derivative **4b**, is the highest, where the three investigated picolinamidines were ordered as **4c** < **4a** < **4b**. The comparison of DFT calculated NMR spectral data with the experimental data showed a good agreement. The *in vitro* antiproliferative data of compounds **4a–c** revealed that the leukemia and colon cancer were the most responsive types of the nine types tested. Picolinamidines **4a** and **4b** exhibited mainly cytotoxic activity, whereas compound **4c** displayed mainly cytostatic activity against leukemia and colon cancer cells. The most active compound was 4-methoxyphenyl derivative **4a** that showed potent antiproliferative activity with GI_{50} values of 0.34 μM, 0.43 μM and 0.88 μM against SR, SW-620 and HT29, respectively. 3,4,5-Trimethoxyphenyl derivative **4c** was less toxic than the other two derivatives. The three compounds were more selective towards the cancer cells while safer to the normal fibroblasts. The tested picolinamidines downregulated the expression of key genes in the cell cycle, *cdk1* and *topoII*, but did not affect the expression of *p53* or *txnrd1*. Compounds **4b** and **4c** caused a significant reduction in the concentrations of Topo II and MAPK proteins. Taken together, these promising anticancer candidates are effective at very low concentrations, safe to normal cells and most probably work through arresting the cell cycle and therefore, they deserve further investigations as potential targeted small anticancer molecules.

Conflicts of interest

The authors declare no conflict of interest.

Acknowledgements

The antiproliferative activity was evaluated at the National Cancer Institute (NCI, USA). This work was supported by the Mansoura research unit, Mansoura University, Egypt [grant number MU-SCI-18-13].

References

1 R. L. Siegel, K. D. Miller and A. Jemal, Cancer statistics, *Ca-Cancer J. Clin.*, 2019, **69**, 7–34.
2 R. L. Siegel, K. D. Miller and A. Jemal, Cancer statistics, *Ca-Cancer J. Clin.*, 2018, **68**, 7–30.
3 L. Xu, L. Shi, S. Qiu, S. Chen, M. Lin, Y. Xiang, C. Zhao, J. Zhu, L. Shen and Z. Zuo, Design, synthesis, and evaluation of cyanopyridines as anti-colorectal cancer agents *via* inhibiting STAT3 pathway, *Drug Des., Dev. Ther.*, 2019, **13**, 3369–3381.
4 M. M. Youssef, R. K. Arafa and M. A. Ismail, Synthesis, antimicrobial, and antiproliferative activities of substituted phenylfuranylnicotinamidines, *Drug Des., Dev. Ther.*, 2016, **10**, 1133–1146.
5 J. K. Thuita, K. K. Wolf, G. A. Murilla, A. S. Bridges, D. W. Boykin, J. N. Mutuku, Q. Liu, S. K. Jones, C. O. Gem, S. Ching, R. R. Tidwell, M. Z. Wang, M. F. Paine and R. Brun, Chemotherapy of Second Stage Human African Trypanosomiasis: Comparison between the Parenteral Diamidine DB829 and Its Oral Prodrug DB868 in Vervet Monkeys, *PLoS Neglected Trop. Dis.*, 2015, **9**, e0003409.
6 J. K. Thuita, K. K. Wolf, G. A. Murilla, Q. Liu, J. N. Mutuku, Y. Chen, A. S. Bridges, R. E. Mdachi, M. A. Ismail, S. Ching, D. W. Boykin, J. E. Hall, R. R. Tidwell, M. F. Paine, R. Brun and M. Z. Wang, Safety, Pharmacokinetic, and Efficacy Studies of Oral DB868 in a First Stage Vervet Monkey Model of Human African Trypanosomiasis, *PLoS Neglected Trop. Dis.*, 2013, **7**, e2230.

7 T. Wenzler, D. W. Boykin, M. A. Ismail, J. E. Hall, R. R. Tidwell and R. Brun, New treatment option for second-stage African sleeping sickness: *in vitro* and *in vivo* efficacy of aza analogs of DB289, *Antimicrob. Agents Chemother.*, 2009, **53**, 4185–4192.

8 L. Hu, R. K. Arafa, M. A. Ismail, T. Wenzler, R. Brun, M. Munde, D. W. Wilson, S. Nzimiro, S. Samyesudhas, K. A. Werbovetz and D. W. Boykin, Azaterphenyl diamidines as antileishmanial agents, *Bioorg. Med. Chem. Lett.*, 2008, **18**, 247–251.

9 M. A. Ismail, W. M. El-Sayed, S. Shaaban, G. A. Abdelwahab and W. S. Hamama, A Review of Cationic Arylfurans and their Isosteres: Synthesis and Biological Importance, *Curr. Org. Chem.*, 2019, **23**, 2751–2782.

10 A. A. Farahat, M. A. Ismail, A. Kumar, T. Wenzler, R. Brun, A. Paul, W. D. Wilson and D. W. Boykin, Indole- and benzimidazole Bichalcophenes: Synthesis, DNA binding and Antiparasitic activity, *Eur. J. Med. Chem.*, 2018, **143**, 1590–1596.

11 S. A. Ohnmacht, E. Varavipour, R. Nanjunda, I. Pazitna, G. Di Vita, M. Gunaratnama, A. Kumar, M. A. Ismail, D. W. Boykin, W. D. Wilson and S. Neidle, Discovery of new G-quadruplex binding chemotypes, *Chem. Commun.*, 2014, **50**, 960–963.

12 M. Munde, A. Kumar, P. Peixoto, S. Depauw, M. A. Ismail, A. A. Farahat, A. Paul, M. V. Say, M. H. David-Cordonnier, D. W. Boykin and W. D. Wilson, The Unusual Monomer Recognition of Guanine-Containing Mixed Sequence DNA by a Dithiophene Heterocyclic Diamidine, *Biochemistry*, 2014, **53**, 1218–1227.

13 R. Nhili, P. Peixoto, S. Depauw, S. Flajollet, X. M. Dezitter, M. Munde, M. A. Ismail, A. Kumar, A. A. Farahat, C. E. Stephens, M. Duterque-Coquillaud, W. D. Wilson, D. W. Boykin and M. H. David-Cordonnier, Targeting the DNA-binding activity of the human ERG transcription factor using new heterocyclic dithiophene diamidines, *Nucleic Acids Res.*, 2013, **41**, 125–138.

14 S. Depauw, M. Lambert, S. Jambon, A. Paul, P. Peixoto, R. Nhili, L. Morongiu, M. Figeac, C. Dassi, C. Paul-Constant, B. Billoré, A. Kumar, A. A. Farahat, M. A. Ismail, E. Mineva, D. P. Sweat, C. E. Stephens, D. W. Boykin, W. D. Wilson and M. David-Cordonnier, Heterocyclic Diamidines DNA ligands as HOXA9 Transcription Factor Inhibitors: Design, Molecular Evaluation and Cellular Consequences in HOXA9-Dependant Leukemia Cell Model, *J. Med. Chem.*, 2019, **62**, 1306–1329.

15 M. A. Ismail, M. M. Youssef, R. K. Arafa, S. S. Al-Shihry and W. M. El-Sayed, Synthesis and antiproliferative activity of monocationic arylthiophene derivatives, *Eur. J. Med. Chem.*, 2017, **126**, 789–798.

16 M. Abdel-Rasol, N. M. El-Beih, S. M. Yahya, M. A. Ismail and W. M. El-Sayed, The antitumor activity of a novel fluorobenzamidine against dimethylhydrazine-induced colorectal cancer in rats, *Anti-Cancer Agents Med. Chem.*, 2020, **20**, 450–463.

17 R. R. Tidwell, D. W. Boykin, C. E. Stephens, M. A. Ismail, A. Kumar, W. D. Wilson and R. Brun and K. Werbovetz, 2,5-Diarylselenophene compounds, aza 2,5-diarylthiophene compounds, and their prodrugs as antiprotozoal agents, *US Pat.*, 2010/0331368A1, December 30, 2010.

18 M. Frisch, G. Trucks, H. Schlegel, G. Scuseria, M. Robb, J. Cheeseman, G. Scalmani, V. Barone, B. Mennucci and G. Petersson, *Gaussian 09, Revision A.1*, Wallingford, CT, 2009.

19 A. D. Becke, Density-functional thermochemistry. III. The role of exact exchange, *J. Chem. Phys.*, 1993, **98**, 5648–5652.

20 C. Lee, W. Yang and R. G. Parr, Development of the Colle-Salvetti correlation-energy formula into a functional of the electron density, *Phys. Rev. B: Condens. Matter Mater. Phys.*, 1988, **37**, 785–789.

21 J. P. Perdew and Y. Wang, Pair-distribution function and its coupling-constant average for the spin-polarized electron gas, *Phys. Rev. B: Condens. Matter Mater. Phys.*, 1992, **46**, 12947–12954.

22 R. Ditchfield, Self-consistent perturbation theory of diamagnetism: I. A Gauge-Invariant LCAO method for NMR chemical shifts, *Mol. Phys.*, 1974, **27**, 789–807.

23 M. Cossi and V. Barone, Time-dependent density functional theory for molecules in liquid solutions, *J. Chem. Phys.*, 2001, **115**, 4708–4717.

24 M. Cossi, N. Rega, G. Scalmani and V. Barone, Energies, structures, and electronic properties of molecules in solution with the C-PCM solvation model, *J. Comput. Chem.*, 2003, **24**, 669–681.

25 R. Dennington, T. Keith and J. Millam, *GaussView, version 5*, Semichem Inc., Shawnee Mission, KS, 2009.

26 D. S. Biovia, *Materials Studio*, Dassault Systèmes, San Diego, 2017.

27 B. Delley, Ground-state enthalpies: evaluation of electronic structure approaches with emphasis on the density functional method, *J. Phys. Chem. A*, 2006, **110**, 13632–13639; B. Delley, An all-electron numerical method for solving the local density functional for polyatomic molecules, *J. Chem. Phys.*, 1990, **92**, 508–517.

28 P. Skehan, R. Storeng, D. Scudiero, A. Monks, J. McMahon, D. Vistica, J. T. Warren, H. Bokesch, S. Kenney and M. R. Boyd, New colorimetric cytotoxicity assay for anticancer-drug screening, *J. Natl. Cancer Inst.*, 1990, **82**, 1107–1112.

29 T. A. McCaffrey, L. A. Agarwal and B. B. Weksler, A rapid fluorometric DNA assay for the measurement of cell density and proliferation *in vitro*, *In Vitro Cell. Dev. Biol.*, 1988, **24**, 247–252.

30 A. Monks, D. Scudiero, P. Skehan, R. Shoemaker, K. Paull, D. Vistica, C. Hose, J. Langley, P. Cronise, A. Vaigro-Wolff, M. Gray-Goodrich, H. Campbell, J. Mayo and M. Boyd, Feasibility of a high-flux anticancer drug screen using a diverse panel of cultured human tumor cell lines, *J. Natl. Cancer Inst.*, 1991, **83**, 757–766.

31 S. A. El-Metwally, A. K. Khalil and W. M. El-Sayed, Design, molecular modeling and anticancer evaluation of thieno [2,3-d]pyrimidine derivatives as inhibitors of topoisomerase II, *Bioorg. Chem.*, 2020, **94**, 103492.

32 K. J. Livak and T. D. Schmittgen, Analysis of relative gene expression data using real-time quantitative PCR and the 2(-delta delta C(T)) method, *Methods*, 2001, **25**, 402–408.
33 M. H. Hekal, A. M. El-Naggar, F. S. M. Abu El-Azm and W. M. El-Sayed, Synthesis of new oxadiazol-phthalazin derivatives with anti-proliferative activity; molecular docking, pro-Apoptotic, and enzyme inhibition profile, *RSC Adv.*, 2020, **10**, 3675–3688.
34 M. A. Ismail, M. H. Abdel-Rhman, G. A. Abdelwahab and W. S. Hamama, Synthesis and spectroscopic studies of methoxysubstituted phenylthienylnicotinamidines, *Synth. Commun.*, 2020, **50**, 2355–2375.
35 B. J. Ramulu, S. Koley and M. S. Singh, Metal-free Brønsted acid mediated synthesis of fully substituted thiophenes *via* chemo-and regioselective intramolecular cyclization of α,α′-bis (β-oxodithioesters) at room temperature, *Org. Biomol. Chem.*, 2016, **14**, 434–439.
36 P. Pouzet, I. Erdelmeier, D. Ginderow, P. M. Dansette, D. Mansuy and J. P. Mornon, Thiophene-1oxides. V. Comparison of the crystal structures and thiophene ring aromaticity of 2,5-diphenylthiophene, its sulfoxide and sulfone, *J. Heterocycl. Chem.*, 1997, **34**, 1567–1574.
37 I. Nohara, A. Prescimone, D. Häussinger, C. E. Housecroft and E. C. Constable, [Cu(POP)(N^S)][PF6] and [Cu(xantphos)(N^S)][PF6] compounds with 2-(thiophen-2-yl)pyridines, *RSC Adv.*, 2019, **9**, 13646–13657.
38 G. Portalone, Benzamidinium 2-methoxybenzoate, *Acta Crystallogr., Sect. E: Struct. Rep. Online*, 2013, **69**, o1114–o1115.
39 D. Sajan, L. Joseph, N. Vijayan and M. Karabacak, Natural bond orbital analysis, electronic structure, non-linear properties and vibrational spectral analysis of L-histidinium bromide monohydrate: a density functional theory, *Spectrochim. Acta, Part A*, 2011, **81**, 85–98.
40 F. A. Bulat, E. Chamorro, P. Fuentealba and A. Toro-Labbe, Condensation of frontier molecular orbital Fukui functions, *J. Phys. Chem. A*, 2004, **108**, 342–349.
41 S. Xavier, S. Periandy and S. Ramalingam, NBO, conformational, NLO, HOMO–LUMO, NMR and electronic spectral study on 1-phenyl-1-propanol by quantum computational methods, *Spectrochim. Acta, Part A*, 2015, **137**, 306–320.
42 M. M. Makhlouf, A. S. Radwan and B. Ghazal, Experimental and DFT insights into molecular structure and optical properties of new chalcones as promising photosensitizers towards solar cell applications, *Appl. Surf. Sci.*, 2018, **452**, 337–351.
43 A. Bouchoucha, S. Zaater, S. Bouacida, H. Merazig and S. Djabbar, Synthesis and characterization of new complexes of nickel(II), palladium(II) and platinum(II) with derived sulfonamide ligand: structure, DFT study, antibacterial and cytotoxicity activities, *J. Mol. Struct.*, 2018, **1161**, 345–355.
44 V. Arjunan, P. Balamourougane, M. Kalaivani, A. Raj and S. Mohan, Experimental and theoretical quantum chemical investigations of 8-hydroxy-5-nitroquinoline, *Spectrochim. Acta, Part A*, 2012, **96**, 506–516.
45 M. Karabacak, M. Cinar and M. Kurt, DFT based computational study on the molecular conformation, NMR chemical shifts and vibrational transitions for *N*-(2-methylphenyl)methanesulfonamide and *N*-(3-methylphenyl)methanesulfonamide, *J. Mol. Struct.*, 2010, **968**, 108–114.
46 M. I. Orief and M. H. Abdel-Rhman, Molecular modeling, spectroscopic and structural studies on newly synthesized ligand *N*-benzoyl-2-isonicotinoylhydrazine-1-carboxamide, *J. Mol. Struct.*, 2018, **1173**, 332–340.
47 Y. Sun, P. Xia, H. Zhang, B. Liu and Y. Shi, P53 is required for doxorubicin-induced apoptosis *via* the TGF-β signaling pathway in osteosarcoma-derived cells, *Am. J. Cancer Res.*, 2016, **6**, 114–125.
48 M. A. Ismail, A. Negm, R. K. Arafa, E. Abdel-Latif and W. M. El-Sayed, Anticancer activity, dual prooxidant/antioxidant effect and apoptosis induction profile of new bichalcophene-5-carboxamidines, *Eur. J. Med. Chem.*, 2019, **169**, 76–88.
49 J. Herrero-Ruiz, M. Mora-Santos, S. Giráldez, C. Sáez, M. Á. Japón, M. Tortolero and F. Romero, βTrCP controls the lysosome-mediated degradation of CDK1, whose accumulation correlates with tumor malignancy, *Oncotarget*, 2014, **5**, 7563–7574.
50 J. J. Liu, Q. Liu, H. L. Wei, J. Yi, H. S. Zhao and L. P. Gao, Inhibition of thioredoxin reductase by auranofin induces apoptosis in adriamycin-resistant human K562 chronic myeloid leukemia cells, *Pharmazie*, 2011, **66**, 440–444.
51 T. Ozaki and A. Nakagawara, p53: the attractive tumor suppressor in the cancer research field, *J. Biomed. Biotechnol.*, 2011, **3**, 994–1013.
52 E. Senturk and J. J. Manfredi, p53 and cell cycle effects after DNA damage, *Methods Mol. Biol.*, 2013, **962**, 49–61.
53 M. Olsson and B. Zhivotovsky, Caspases and cancer, *Cell Death Differ.*, 2011, **18**, 1441–1449.
54 J. M. Enserink and R. D. Kolodner, An overview of Cdk1-controlled targets and processes, *Cell Div.*, 2010, **5**, 1–41.
55 E. S. Arnér and A. Holmgren, Physiological functions of thioredoxin and thioredoxin reductase, *Eur. J. Biochem.*, 2000, **267**, 6102–6109.
56 P. Nguyen, R. T. Awwad, D. D. Smart, D. R. Spitz and D. Gius, Thioredoxin reductase as a novel molecular target for cancer therapy, *Cancer Lett.*, 2005, **2361**, 64–74.
57 K. F. Tonissen and G. Di Trapani, Thioredoxin system inhibitors as mediators of apoptosis for cancer therapy, *Mol. Nutr. Food Res.*, 2009, **53**, 87–103.
58 G. Ambrosini, H. S. Cheema, S. Seelman, E. B. Sambol, S. Singer and G. K. Schwartz, Sorafenib Inhibits Growth and MAPK Signaling in Malignant Peripheral Nerve Sheath Cells, *Mol. Cancer Ther.*, 2008, **7**, 890–896.
59 J. L. Nitiss, Targeting DNA topoisomerase II in cancer chemotherapy, *Nat. Rev. Cancer*, 2009, **9**, 327–337.
60 E. Willmore, S. de Caux and N. J. Sunter, A novel DNA-dependent protein kinase inhibitor, NU7026, potentiates the cytotoxicity of topoisomerase II poisons used in the treatment of leukemia, *Blood*, 2004, **103**, 4659–4665.

